Available online at www.sciencedirect.com
ScienceDirect
Journal of Applied Mathematics and Mechanics 70 (2006) 446–458
Journal of APPLIED MATHEMATICS AND MECHANICS
www.elsevier.com/locate/jappmathmech

The indentation of a spherical punch into an ideally plastic half-space when there is contact friction☆

R.I. Nepershin

Moscow

Received 6 January 2005

Abstract

Calculations are presented of the indentation of a spherical punch into an ideally plastic half-space under condition of complete plasticity and taking account of contact friction, which is modelled according to Prandtl and Coulomb. Friction leads to the formation of a rigid zone at the centre of the punch when there is slipping of the material on the remaining part of the contact boundary. Limit values of the friction coefficients are obtained for which the rigid zone extends over the whole of the contact boundary. The dependence of the indentation force on the radius of the plastic area is in good agreement with experimental data.

The solution of an axisymmetric problem of ideal plasticity concerning the stress distribution in a plastic region accompanying the pressure of smooth flat and spherical punches on a plastic half-space with a linear boundary was presented in Refs. 1–3. The velocity fields of a plastic flow, which satisfy the condition of non-negative energy dissipation, were calculated and a statically admissible continuation of the stress fields into the rigid zone in the problem of the pressure of a smooth spherical punch on a half-space with a linear boundary was pointed out.[3,4] The results of the modelling of the unsteady process of the indentation of a smooth spherical punch into an ideally plastic half-space were presented and the shape of the free boundary of the plastic region around the punch was calculated.[5] In the case of a smooth punch and large indentation radii, the calculated dependence of the indentation force on the radius of the plastic area is found to be lower than the experimental dependence[6] as a consequence of the effect of contact friction.

Calculations of the unsteady process of plastic flow accompanying the indentation of a spherical punch into an ideally plastic half-space when there is contact friction are presented below. Unlike the problems considered earlier,[1–6] the model presented shows the formation of a rigid zone of the material in front of the punch, which depends on the friction. When contact friction is taken into account one obtains better correlation between the calculated dependence of the indentation force for a spherical punch on the radius of the plastic area and the experimental data[6] compared with the indentation of a smooth spherical punch.[1–5]

1. Formulation of the problem and basic equations

Consider the indentation of a spherical punch into an ideally plastic half-space in cylindrical coordinates r, z, θ, associated with the moving punch, with origin of coordinates at the lowest point of the punch. In these coordinates,

☆ *Prikl. Mat. Mekh.*, Vol. 70, No. 3, pp. 490–503, 2006.

E-mail address: nepershin_r@pop.mtu.ru.

0021-8928/$ – see front matter © 2006 Elsevier Ltd. All rights reserved.
doi:10.1016/j.jappmathmech.2006.07.011

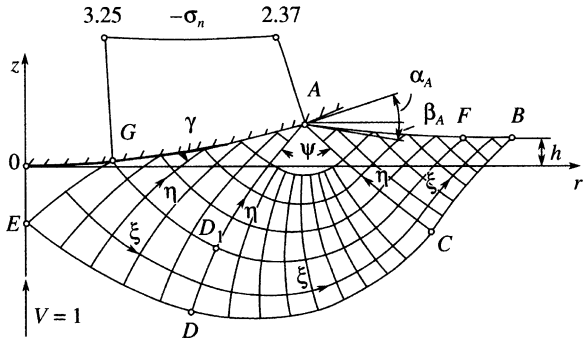

Fig. 1.

the punch is fixed and the half-space moves along the z axis with the indentation velocity, which we will adopt as the characteristic velocity of the problem and put equal to unity ($V=1$).

The form of the plastic region to the right of the axis of symmetry is shown in Fig. 1 for the case of the indentation of a punch of radius R to a depth h relative to the undeformed horizontal boundary of the half-space. We will specify the current stage of indentation by the angle α_A of the arc of contact of the punch with the plastic region. Since, at the time of indentation, the plastic region has dimensions of the order of the length of the contact arc, we will adopt the length of the contact arc $R\alpha_A = 1$ as the characteristic dimension when calculating the plastic flow for the current stage of indentation. In modelling the indentation process from the beginning of the contact between the punch and the half-space up to the final depth of penetration with a radius of the plastic area $R\sin\alpha_A$, we will adopt the radius of the punch $R=1$ as the characteristic dimension. We will also assume that the stresses are dimensionless, having been divided by the yield stress of the material α_Y under uniaxial compression.

Assuming Tresca plasticity, three-dimensional plastic deformation of an isotropic, ideally plastic material occurs with shearing along two slip planes, during which the stress state corresponds to the condition of complete plasticity which, in the problem being considered, has the form

$$\sigma_1 = \sigma_2, \quad \sigma_3 = \sigma_1 - 1 \tag{1.1}$$

in the space of the principal stresses.

The directions of the principal stresses σ_1 and σ_3 lie in the $\{r, z\}$ plane and σ_2 is identical to the peripheral stress σ_θ. In the case of condition (1.1), an axisymmetric problem of ideal plasticity is statically determinate and hyperbolic.[3] The characteristics for the stresses and displacement rates coincide with the slip lines ξ and η in the $\{r, z\}$ plane,

$$dz/dr = \operatorname{tg}\varphi \text{ для } \xi \text{ и } dz/dr = -\operatorname{ctg}\varphi \text{ для } \eta \tag{1.2}$$

where φ is the angle between the tangent to the slip line ξ and the r axis. The differential relations for $\sigma = (\sigma_1 + \sigma_3)/2$ and φ

$$d\sigma - d\varphi = \frac{dr + dz}{2r} \text{ along } \xi, \quad d\sigma + d\varphi = \frac{dr - dz}{2r} \text{ along } \eta \tag{1.3}$$

are satisfied along the slip lines and, in the case of the projections V_ξ, and V_η of the velocity vector for displacement onto the slip lines ξ and η,

$$dV_\xi - V_\eta d\varphi = -\frac{V_\xi dr - V_\eta dz}{2r} \text{ along } \xi, \quad dV_\eta + V_\xi d\varphi = -\frac{V_\xi dz + V_\eta dr}{2r} \text{ along } \eta \tag{1.4}$$

The displacement rates in cylindrical coordinates are connected with V_ξ and V_η by the relations

$$\begin{aligned} V_\xi &= V_r\cos\varphi + V_z\sin\varphi, \quad V_\eta = V_z\cos\varphi - V_r\sin\varphi \\ V_r &= V_\xi\cos\varphi - V_\eta\sin\varphi, \quad V_z = V_\xi\sin\varphi + V_\eta\cos\varphi \end{aligned} \tag{1.5}$$

The differential relations (1.4) allow of discontinuities in the displacement rates V_ξ and V_η along the slip lines ξ and η which, unlike the constant discontinuities in the rates under plane deformation, are variable owing to the inhomogeneity

of relation (1.4) and are given by the expressions.[7–9]

$$[V_\xi] = \frac{C_1}{\sqrt{r}}, \quad [V_\eta] = \frac{C_2}{\sqrt{r}} \tag{1.6}$$

The constants C_1 and C_2 are determined by the kinematic boundary conditions of the problem.

In Prandtl and Hill problems on the indentation of punches accompanying plane deformation, the kinematic joining of the rigid and plastic regions leads to constant discontinuities along the rigid - plastic boundaries. In axisymmetric problems on the indentation of punches with a plastic region containing an axis of symmetry, when $C_1 \neq 0$ or $C_2 \neq 0$ the discontinuities in the velocities along the rigid - elastic boundaries increase without limit as $r \to 0$. In order to preclude an unlimited increase in the velocities on the axis of symmetry, it is assumed that $C_1 = C_2 = 0$, which corresponds to continuity of the velocities on the rigid - plastic boundaries. Kinematic joining of rigid zones, which have different velocities and bounded slip lines with a common point on the axis of symmetry, is achieved using the self-similar singular solution in a small neighbourhood of the point of intersection of the rigid - plastic boundaries with the axis of symmetry.[7–9]

The condition for the rate of dissipation of energy of the plastic flow to be non-negative

$$D = \sigma_1\varepsilon_1 + \sigma_2\varepsilon_2 + \sigma_3\varepsilon_3 \geq 0 \tag{1.7}$$

must be satisfied in the plastic region, where ε_1, ε_2 and ε_3 are the principal strain rates. In the case of complete plasticity (1.1), the inequality $\varepsilon_3 \leq 0$ follows from condition (1.7) and the incompressibility condition $\varepsilon_1 + \varepsilon_2 + \varepsilon_3 = 0$, which shows that the dissipative function is non-negative if the rate of elongation of a linear element along the trajectory of the stress σ_3 is negative. In curvilinear coordinates associated with the directions of the principal stresses σ_3 and σ_1, this equality has the form

$$dV_3 - V_1 d\varphi \leq 0 \tag{1.8}$$

where $d\varphi$ is the angle of rotation of the tangent to the element of an arc of the trajectory of the stress σ_3, V_3 and V_1 are the projections of the velocity vector onto the directions σ_3 and σ_1 which are connected with V_ξ and V_η by the relations

$$V_3 = (V_\xi - V_\eta)/\sqrt{2}, \quad V_1 = (V_\xi + V_\eta)/\sqrt{2} \tag{1.9}$$

Inequality (1.8) is easily verified by numerical modelling of the indentation of a punch and displaying the slip lines in the physical $\{r, z\}$ plane and the displacement velocity fields in the plane of the hodograph $\{V_r, V_z\}$ on the screen of a monitor.

In the case of a smooth punch, the boundary of contact with the plastic region extends along the whole arc $R\alpha_A$ and the slip lines intersect this boundary at an angle of $\pi/4$. Friction at the contact boundary leads to the formation of a rigid zone in the central part of the punch, which is bounded by the slip line η that intersects the axis of symmetry at the point E at an angle of $\pi/4$ and the boundary of the punch at point G at an angle which depends on the contact friction shear stress. This region is an "outgrowth" of the material in front of the punch, which is observed in practice and is used to estimate the friction coefficient experimentally.[10]

Slip of the plastic material along the punch boundary, with shear stresses which depend on the friction law, occurs on the remaining part of the contact arc. In this paper, the Prandtl and Coulomb models of contact friction are used. According to the Prandtl model, the shear stress of contact friction is assumed to be a constant of magnitude μ and is treated as a resistance to shearing of the contact layer, which depends on the lubricant, the state of the surface and other factors. The value of μ is limited by the shear yield point of the plastic material and can vary over a range $0 < \mu < 1/2$. Prandtl friction is usually employed in technological problems in the theory of plasticity in the case of high contact pressures.[10,11] When modelling Coulomb contact friction, the shear stresses are calculated together with the unknown normal stresses. The range of values of the Coulomb friction coefficient is found below; in this range the mean contact shear stress for a specified value of f is close to the value of μ, and the stress and velocity plastic flow fields for the Prandtl and Coulomb models are close to one another.

We will model the indentation of a punch into a half-space by a sequence of loading steps, changing the angle of the contact arc α_A from zero to the limit value, during which the structure of the field of the slip lines, shown in Fig. 1, is preserved. For each step in the loading, we will calculate the free boundary AB, and the shape and dimensions of the plastic region in the case of the boundary conditions for the stresses and displacement velocities cited below.

2. Boundary conditions

We will write the equation of the punch boundary OA (Fig. 1) in the parametric form

$$r = \sin\alpha/\alpha_A, \quad z = (1-\cos\alpha)/\alpha_A, \quad 0 \le \alpha \le \alpha_A \tag{2.1}$$

where α_A is the angle of inclination of the tangent at point A to the contact arc OA, which is adopted as a characteristic dimension $R\alpha_A = 1$. When there is friction, the slip lines η intersect the contact boundary at an angle γ, which can vary from zero in the case of a perfectly rough punch to $\pi/4$ in the case of a perfectly smooth punch. The shear stress τ and the normal pressure p on the slip boundary AG are given by the relations

$$\tau = \frac{1}{2}\cos 2\gamma, \quad p = \frac{1}{2}\sin 2\gamma - \sigma \tag{2.2}$$

where σ is the mean stress, which occurs in expressions (1.3), and the angles γ, φ and α are connected by the relation

$$\gamma = \varphi - \alpha + \pi/2 \tag{2.3}$$

In modelling the Prandtl contact friction, we specify that $\tau = \mu$, $(0 < \mu < 1/2)$, we find the angle γ from the first relation of (2.2) and we find the angle φ at points of the slip boundary AG, which are specified by the angle α in relations (2.1). In modelling Coulomb contact friction, we specify the friction coefficient f and, from expressions (2.2) and (2.3), we obtain the non-linear relation between σ and φ

$$f(2\sigma + \sin 2(\varphi - \alpha)) - \cos 2(\varphi - \alpha) = 0 \tag{2.4}$$

Provided there is complete plasticity (1.1), the boundary AB of the plastic region, which is, free from external stresses, finds itself in a state of uniaxial compression and coincides with the direction of the principal stress σ_3

$$\sigma_1 = \sigma_2 = 0, \quad \sigma_3 = -1 \tag{2.5}$$

The calculations of the velocity fields of the initial axisymmetric plastic flow accompanying the indentation of punches into a half-space [3,4,8,9] show an increase in the velocities of points in the free horizontal boundary AB from point B to point A, which lead to the inclined rising and distortion of the free boundary of the plastic region around a spherical punch, which is observed experimentally.[6]

In this paper, in modelling the unsteady indentation of a spherical punch, we assume that the boundary AB is a smooth curve with a continuous change in the angle of inclination of the tangent from a maximum value β_A at point A to zero at point B as a consequence of the continuity in the change in the displacement velocities along the rigid-plastic boundary $BCDE$. The boundary conditions on AB for differential relations (1.2) and (1.3)

$$\sigma = -1/2, \quad \varphi = \pi/4 - \beta, \quad \beta = -\operatorname{arctg}(dz/dr) \text{ on } AB \tag{2.6}$$

follow from relations (2.5).

Since the boundary AB of the current stage of indentation is formed by point masses which are displaced from the boundary $A'B'$ of the preceding stage of indentation, the differential relation for the displacements

$$ds/V = dh \text{ in } AB \tag{2.7}$$

must be satisfied on this boundary, where ds is the mean modulus of the vector of the displacement of a point to the current boundary AB from the preceding boundary $A'B'$ after a "time" dh, V is the mean modulus of the velocity vector of the point being considered after a "time" dh, and dh is the increment in the depth of indentation $h = z_B$. As a consequence of the incompressibility of the plastic material, the volume which is forced out by a spherical segment of a punch of height h is equal to the volume of the plastic region above the boundary $z = z_B$. The relation between h and the free boundary AB of the plastic region

$$h = \frac{1}{r_B^2}\left[z_A\left(r_A^2 - \frac{1}{3}z_A^2\right) + 2\int_A^B z r dr\right]; \quad r_A = \frac{\sin\alpha_A}{\alpha_A}, \quad z_A = \frac{1-\cos\alpha_A}{\alpha_A} \tag{2.8}$$

follows from this condition, where r_A and z_A are the coordinates of point A.

Point A is a degenerate ξ-slip line with a polar singularity in the change of the stresses and displacement velocities within the limits of the angle ψ of the centred fan

$$\psi = \frac{3}{4}\pi - (\alpha_A + \beta_A + \gamma) \tag{2.9}$$

The inequality $\psi > 0$ defines the limit value of the contact angle α_A and the depth of indentation of the punch h for which the field of slip lines in the plastic region has the form shown in Fig. 1. From the first relation of (1.3) at the singular point A and the boundary condition (2.6), we find σ and φ at this point

$$\sigma = -(1/2 + \zeta), \quad \varphi = \pi/4 - (\beta_A + \zeta), \quad 0 \le \zeta \le \psi \tag{2.10}$$

In the Prandtl model of contact friction, we find the angle γ, which determines the centred fan according to relation (2.9) for specified α_A and β_A from the first relation of (2.2) when $\tau = \mu$. In the Coulomb model of contact friction, from relations (2.2), (2.9) and (2.10) when $\xi = \psi$, we obtain the following non-linear equation for the angle γ at point A on the boundary of contact of the punch with the plastic region

$$\cos 2\gamma + f\left(2\left(\gamma + \alpha_A + \beta_A - \frac{1}{2} - \frac{3}{4}\pi\right) - \sin 2\gamma\right) = 0 \tag{2.11}$$

We will solve Eq. (2.11) by Newton's iterative method.

For a smooth punch, the slip boundary GA coincides with the whole of the contact boundary OA and the central rigid zone shrinks to the point O. On the other hand, there are limit values of the friction coefficients μ^* and f^* for which the slip boundary GA shrinks to the point A, and point D coincides with point E on the axis of symmetry (Fig. 1).

We will determine the limit friction coefficients from the conditions that point D should be on the axis of symmetry which the slip lines intersect at angle of $\pi/4$. In the case of a known free boundary AB of the plastic region, we find the coordinates of point D and the angle φ at this point from the solution of a Cauchy problem in the domain ABC for the differential relations (1.2) and (1.3) and the boundary conditions (2.6) and a Goursat problem in the domain ACD for the slip line AC and the singular point A with an angle of the centred fan ψ. In this case, the rigid-plastic boundary BCD is determined by the coordinates of point B and the angle ψ. As a result, we obtain two functional equations which determine the boundary conditions at point D

$$r_D(\psi, \mathbf{r}_B) = 0, \quad \varphi_D(\psi, \mathbf{r}_B) + \pi/4 = 0 \tag{2.12}$$

where $\mathbf{r}_B$ is the radius vector of point B. We find the angle ψ from these equations and the limit angle γ^* at point A from relation (2.9). Then, from the first relation of (2.2), we find μ^* in the case of the Prandtl model of friction and, from (2.11), we find f^* in the case of the Coulomb model.

If the friction coefficients satisfy the inequalities

$$0 < \mu < \mu^* \quad \text{or} \quad 0 < f < f^* \tag{2.13}$$

we then determine the boundary EG of the central rigid zone. In this case, we find the angle $\gamma > \gamma^*$ at point A from the first relation of (2.2) in the case of Prandtl friction, and from Eq. (2.11) in the case of Coulomb friction, and we find the angle ψ from relation (2.9). We find the plastic region with the rigid-plastic boundaries EG and $BCDE$ from the solution of the sequence of boundary-value problems for the differential relations (1.2) and (1.3), which are Cauchy problems in the domain ABC, Goursat problems in the domain ACD, problems of a mixed type in the domain AD_1G with the boundary conditions on the slip boundary AG and Goursat problems in the domain DD_1GE. The conditions that point E should fall on the axis of symmetry leads to two functional equations for the coordinates of points F and B on the free boundary AB

$$r_E(\mathbf{r}_B, \mathbf{r}_F) = 0, \quad \varphi_E(\mathbf{r}_B, \mathbf{r}_F) + \pi/4 = 0 \tag{2.14}$$

where $\mathbf{r}_B$ and $\mathbf{r}_F$ are the radius vectors of points B and F.

As a consequence of relation (2.7), the free boundary AB is related to the kinematic plastic flow determined by the differential relations (1.4) and the boundary conditions for the displacement velocities presented below.

The displacement velocities are continuous on the rigid-plastic boundaries since these boundaries intersect the axis of symmetry. On the boundary EG with the fixed central rigid zone, we have the condition

$$V_\xi = V_\eta = 0 \quad \text{on} \quad EG \tag{2.15}$$

The displacement velocities $V_r = 0$ and $V_z = 1$ are specified on the boundary $BCDE$ of the half-space with the rigid zone. From the first of relations (1.5), we find

$$V_\xi = \sin\varphi, \quad V_\eta = \cos\varphi \quad \text{on} \quad BCDE \tag{2.16}$$

On the slip boundary AG, the component of the velocity vector which is normal to the boundary is continuous, and the boundary condition

$$V_\xi = V_\eta \operatorname{tg}\gamma \quad \text{on} \quad AG \tag{2.17}$$

follows from this, where the angle γ is the angle of inclination of the slip line η to the boundary of the punch, which is related to the angles φ and α by relation (2.3).

3. Numerical solution

In modelling the indentation of a spherical punch, the technique for calculating the unknown free boundary AB of the half-space around the punch which, as a consequence of the hyperbolic character and static determinacy of the differential equations for axisymmetric plastic flow, determines the stress and displacement velocity fields in the plastic region using the boundary conditions presented in Section 2, is a fundamental problem in the algorithm for its numerical solution.

Calculation of the boundary AB from differential relation (2.7) using the numerical results of calculations of the slip lines and displacement velocities on the boundary $A'B'$ obtained at the preceding stage of the indentation of the punch for a specified step size dh leads to the following difficulties.

To calculate the new boundary AB correctly using the known preceding boundary $A'B'$, it is necessary to take account of the rapid change in the boundaries of the plastic region and the displacement velocity fields accompanying the punch indentation step dh, especially at the first stage of the indentation starting from the point contact of the punch with the half-space. As a consequence of the singularity of the slip lines and the displacement velocity fields at the singular point A', the calculation of the new point of contact A of the punch with the free boundary of the plastic region represents a difficult problem. As a consequence of errors in the numerical calculation of the nodal points of the slip lines and the displacement velocities, which accumulate when solving the sequence of boundary-value problems, the boundary AB which is calculated is inaccurate and piecewise-linear. Continuation of the calculations of the slip lines and displacement velocities from this boundary on further indentation of the punch is only possible after smoothing it out with a continuous curve.

In this paper, the unsteady indentation of a spherical punch taking account of contact friction, is modelled using a semi-inverse method for calculating the free boundary of the plastic region, was used earlier in Ref. 5. We will assume that the free boundary AB is a smooth curve with a monotonic decrease in the angle of inclination of the tangent β from its maximum value β_A at point A on the boundary of the punch to zero at point B on the boundary of the half-space. This assumption agrees with the velocity distribution on the free boundary of the half-space in problems concerning an initial plastic flow and with the experimental data which have been discussed above.

We will model the indentation process with an increasing sequence of values of the contact angle α_A from zero to a finite value, which satisfies the inequality $\psi > 0$ for the centred fan of slip lines at point A. Here, the singular point A is defined by relations (2.1) and corresponds to the specification of the radius of the plastic area, while the corresponding value of the indentation depth h is found after calculating the boundary AB and the numerical solution, with a check of the error of the differential relation (2.7) at points of the free boundary.

We will approximate the change in the angle of inclination of the tangent β on the free boundary AB by a power dependence on the radius

$$\beta = \beta_A(1 - \rho^n), \quad \rho = (r - r_A)/(r_B - r_A) \tag{3.1}$$

where r_A and r_B are the radial coordinates of points A and B. The parameter n in relation (3.1) enables us to change the curvature of the boundary AB in order to satisfy the kinematic condition (2.7) more accurately. From relations (3.1), we find the dependence of r on β from the condition $r = r_A$ when $\beta = \beta_A$

$$r = r_A + (r_B - r_A)\exp\{n^{-1}\ln(1 - \beta/\beta_A)\}, \quad 0 \le \beta < \beta_A \tag{3.2}$$

We calculate the boundary AB by numerical integration of the equation

$$dz/dr = -\mathrm{tg}\beta \tag{3.3}$$

using relations (3.1) and (3.2) for a uniform step size with respect to the angle β and specified values of the parameters r_B, β_A and n. The coordinate z_B of point B is equal to the indentation depth h.

We find the angle β_A at point A from the integral incompressibility condition (2.8) by Newton's iterative method, while treating expression (2.8) as an implicit function of β_A. In the initial approximation, $\beta_A^0 = 0.8\alpha_A$ and the angle β_A is determined with an accuracy of 10^{-4} practically instantaneously.

We find the slip line and displacement velocity fields by numerical solution of a sequence of boundary-value problems of the Cauchy, Goursat and mixed type, starting from the free boundary AB for an increasing sequence of values of the contact angle d_A from zero to a finite value, which satisfies the inequality $\psi > 0$. At regular nodes of the mesh of slip lines, which do not belong to boundaries, we calculate the coordinates of the nodes and the values of the functions σ and φ by an iterative method.[8,9]

After integrating Eq. (3.3), the radius vector of point B is determined for a specified value of the coordinate r_B, and the system of equations (2.12) for determining the limit friction coefficients depends on the two scalar variables ψ and r_B. Since the equations for an axisymmetric flow are determined subject to the condition that $r > 0$, a numerical solution of system (2.12) cannot be successfully obtained using standard methods, since the functional matrix of this system when $r \to 0$ turns out to be ill-posed. The solution of system (2.12) was found by varying the values of r_B in the initial data of the computational program and solving the second equation of (2.12) for the variable ψ using Newton's method with an accuracy of 10^{-4}. The first equation of (2.12) is solved with an accuracy of $\sim 10^{-4}$ for values of r_B specified with an accuracy of 10^{-4}.

If the friction coefficients are less than the limit values, then, on the slip boundary AG, we calculate a sequence of nodal points which satisfy boundary conditions (2.3) or (2.4) when modelling Prandtl or Coulomb contact friction respectively. Point 1, on the ξ-slip line close to the punch boundary, at which σ and φ are known, is shown in Fig. 2 as well as the point P of the intersection of this line with the punch boundary, at which σ and φ are unknown. On replacing the first equation of (1.2) and the first relation of (1.3) by finite differences between the points 1 and P, we obtain the relations

$$z_1 - z = (r_1 - r)\mathrm{tg}\hat{\varphi}, \quad \hat{\varphi} = (\varphi + \varphi_1)/2 \tag{3.4}$$

$$\sigma = \sigma_1 + \varphi - \varphi_1 - (r_1 - r + z_1 - z)/(r_1 + r) \tag{3.5}$$

where known quantities at point 1 are labelled with the subscript 1. The coordinates r and z of point P and the angle φ at this point are determined by relations (2.1) and (2.3).

When modelling Prandtl friction, the angle γ in relation (2.3) is determined by the friction coefficient $\mu = \tau$ from the first relation of (2.2). In this case, substitution of expressions (2.1) and (2.3) into relations (3.4) leads to a transcendental equation for the angle α, which determines the coordinates of the point P on the punch boundary

$$\begin{aligned} &(r_1 - \sin\alpha/\alpha_A)\mathrm{tg}\hat{\varphi} + (1 - \cos\alpha)/\alpha_A - z_1 = 0 \\ &\hat{\varphi} = (\alpha + \gamma + \varphi_1 - \pi/2)/2 \end{aligned} \tag{3.6}$$

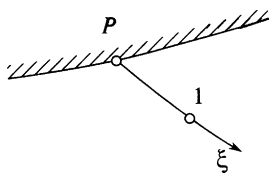

Fig. 2.

Equation (3.6) was solved with an accuracy of 10^{-4} using Newton's method. The initial approximation α^0 was found from equation (2.1) for the point of intersection of the punch boundary with the straight line which passes through point 1 with an angle of inclination φ_1. From relations (2.1), (2.3) and (3.5) we next find the coordinates of the point P and the magnitudes of φ and σ at this point.

When modelling internal Coulomb friction, from relations (2.4), (3.4) and (3.5) we obtain the following system of non-linear equations for φ and α at the point P

$$\Delta z - \Delta r \operatorname{tg}\hat{\varphi} = 0 \tag{3.7}$$

$$\frac{1}{2}(f^{-1}\cos\theta - \sin\theta) - \sigma_1 - \varphi + \varphi_1 + (\Delta r + \Delta z)/(r_1 + r) = 0 \tag{3.8}$$

where

$$\Delta r = r_1 - r, \quad \Delta z = z_1 - z, \quad \hat{\varphi} = \frac{1}{2}(\varphi + \varphi_1), \quad \theta = 2(\varphi - \alpha)$$

and the coordinates r and z at the point P are determined by relations (2.1) in terms of the angle α. Equations (3.7) and (3.8) were solved using Broyden's method[12] with an accuracy of 10^{-4} using the values of φ and α from the preceding mesh points on the punch boundary, beginning from point A, as the initial approximation. The value of σ at the point P was then found from relation (2.4).

The radius vectors of points B and F, which determine the boundary of the plastic region and the slip boundary AG by relations (2.14), were found by integrating differential equation (3.3) during calculations of the free boundary AB, specifying the coordinates of r_B and r_F of these points. Equations (2.14) were solved with an accuracy of $\sim 10^{-4}$ by varying the values of r_B and r_F in the initial data of the computational program.

After the slip line fields have been calculated, the rigid-plastic boundaries, on which the boundary conditions (2.15)–(2.17) are specified for the displacement velocities, are determined. The numerical solution of differential relations (1.4) with boundary conditions (2.15) and (2.16), using the finite-difference relations presented earlier in Ref. 8, gives a linear system of equations for the displacement velocities at the regular nodes of the slip line mesh.

The second differential relation of (1.4) and boundary condition (2.17) were used to calculate the displacement velocities at the mesh points on the slip boundary AG. Point *2* on the η-slip line close to the punch boundary, at which the displacement velocities are known, and the point P of the intersection of this line with the punch boundary are shown in Fig. 3. Approximating the second differential relation of (1.4) by finite differences between the points 1 and P, we obtain

$$V_\eta - V_{\eta 2} + \frac{1}{2}(V_\xi + V_{\xi 2})(\varphi - \varphi_2) + \frac{1}{2}[(V_\xi + V_{\xi 2})\Delta z + (V_\eta + V_{\eta 2})\Delta r]/(r + r_2) = 0 \tag{3.9}$$

where

$$\Delta r = r - r_2, \quad \Delta z = z - z_2$$

and known quantities at point *2* are labelled with the subscript 2. Since the coordinates r and z and the angle φ are known after determining the slip lines at points on the punch boundary, relation (3.9) together with boundary condition (2.17) form a linear system of equations from which we find the velocities V_ξ and V_η on the slip boundary AG. After solving the boundary-value problems for the displacement velocity fields, we obtain the velocities at the mesh points on the free boundary AB

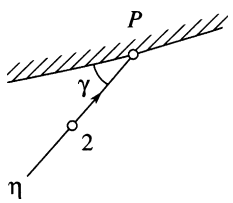

Fig. 3.

For a small indentation depth h, the left-hand and right-hand sides of kinematic condition (2.7) are of the order of 10^{-3}, the angles α_A and β_A are small and the boundary AB is almost linear. For a value of the parameter $n = 1.65$ in relation (3.1) in the case of the maximum Prandtl and Coulomb friction coefficients for the contact angles $\alpha_A = 0.3$ and $\alpha_A = 0.25$ a mean relative error in condition (2.7) of $\sim 10^{-2}$ and a maximum relative error of $\sim 10^{-1}$ was obtained for an increment in the indentation depth $\Delta h = 0.0488$. Hence, when the angles of inclination of the tangent at the mesh points of the free boundary AB are approximated relation (3.1), we obtain an error in violating differential kinematic condition (2.7) which is commensurate with the error in the numerical calculations of the slip line fields and the velocity fields. It is possible that the use of other methods of approximating the free boundary AB can reduce the error associated with the violation of condition (2.7).

We find the indentation force of the punch Q by numerical integration of the stress distribution on the rigid-plastic boundary EG and on the slip boundary AG

$$Q = 2\pi\left[\int_E^G r\left[(-\sigma)dr + \frac{1}{2}dz\right] + \int_G^A r\left[\left(\frac{1}{2}\sin 2\gamma - \sigma\right)dr + \frac{1}{2}\cos 2\gamma dz\right]\right] \tag{3.10}$$

Since the problem being considered is of practical interest in hardness testing by impressing a rigid sphere into plastic metals, the dimensionless Meyer's numbers q_M (the mean pressure for the projection of the plastic area onto a plane perpendicular to the z axis) and Brinell's numbers q_B (the mean pressure on the plastic area) were also calculated.

$$q_M = Q/(\pi r_A^2), \quad q_B = Q/[\pi(r_A^2 + z_A^2)] \tag{3.11}$$

4. Numerical results

The results of calculations of the limit Prandtl and Coulomb friction coefficients μ^* and f^* as a functions of the contact angle α_A and the corresponding values of the relative indentation depth h/R, the relative radius of the plastic indentation r_A/R and the dimensionless hardness numbers q_M and q_B are presented below

α_A	0	0.05	0.1	0.15	0.2	0.25	0.3
$\mu^* \cdot 10^3$	397	425	452	473	488	496	500
$f^* \cdot 10^3$	146	169	180	190	196	200	203
$(h/R) \cdot 10^4$	0	9	35	79	141	221	317
$(r_A/R) \cdot 10^3$	0	50	100	149	199	247	295
q_M	3.026	3.014	3.003	2.991	2.979	2.969	2.957
q_B	3.026	3.012	2.995	2.975	2.949	2.957	2.891

When $\alpha_A \to 0$ (the indentations of a flat circular punch without slip of the material along the boundary of contact), the results of the calculations agree with those obtained earlier in Ref. 13.

The value of the coefficient μ^* is equal to the shear stress on the boundary of the punch at point A. The value of the coefficient f^* is equal to the ratio of the shear stress to the normal pressure on the boundary of the punch at point A.

It can be seen that, for a small indentation depth, the limit friction coefficients μ^* have high values, which are close to the corresponding values for a perfectly rough punch. If the friction coefficient lies in the interval of limit values, then, at the initial stage of the indentation of the punch up to the corresponding value of the contact angle α_A or the radius of plastic area, the central rigid zone extends to the whole boundary of contact. When the punch is impressed further, the central rigid zone will only extend to a part of the boundary of contact with the punch, and the slip boundary AG appears.

The slip lines in the $\{r, z\}$ plane and their mapping onto the plane of the hodograph of the displacement velocities V_r and V_z for a contact angle $\alpha_A = 0.3$ at which the friction coefficient μ^* takes a limit value of 0.5 are shown in Figs. 4 and 5. In this case, the boundary AD of the central rigid zone is directed along the tangent to the boundary of the punch at point A. When the punch is impressed further when $\alpha_A > 0.3$, a slip boundary appears around the point A, which will be the envelope for the slip lines of the family η.

As a consequence of the change in the velocity V_z from unity to zero at point D, a singular displacement velocity field, which has been presented earlier in Ref. 13, arises in the neighbourhood of this point. Owing to this, a rapid

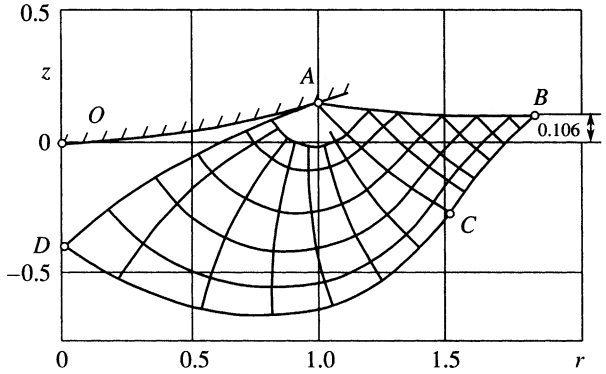

Fig. 4.

change in the velocity is obtained along the slip lines closest to the rigid-plastic boundaries AD and BCD. The plastic region ABC (Fig. 4) is mapped onto the plane of the velocity hodograph (Fig. 5) by a narrow segment with a reduction in the velocity V_3 along the trajectory of the principal stress σ_3, with which the boundary AB coincides. In the plastic region in the physical plane (Fig. 4), the curvature of the trajectories of the principal stress σ_3 is positive ($d\varphi > 0$), the projections of the velocity vector V_3 and V_1 are positive and V_3 decreases along the trajectories of σ_3 (Fig. 5). The inequality (1.7) is satisfied over the whole of the plastic region and the dissipative function D is positive. The statically allowable continuation of the stresses into the rigid zone in the case of the slip line field accompanying the indentation of a spherical punch has been presented earlier in Ref. 3.

An example of the calculation of a slip line field when a punch is indented up to a contact angle $\alpha_A = 0.3$ for $\mu = 0.3$ with a distribution of the normal pressure σ_n on the slip boundary AG, which increases from 2.372 at point A to 3.253 at point G is shown in Fig. 1. In this example, the indentation depth and the mean pressures on the punch are given by the equalities $h/R = 0.03$, $q_M = 2.878$ and $q_B = 2.814$.

When testing the hardness of metals by indenting a sphere and when developing machine components with plastic deformation of the surface layer with a spherical indentor, the friction coefficients are considerably less than the limit values presented at the beginning of this section. In these processes, a central rigid zone is formed from the very beginning of the indentation of the punch and also a slip boundary AG in accordance with the scheme shown in Fig. 1.

The results of calculations of the relative values of the indentation depth of the punch h/R, of the depth of the central rigid zone on the axis of symmetry $-z_E/R$, the radial boundary of the central rigid zone on the punch surface r_G/R and the dimensionless hardness numbers are presented in Table 1 as a function of the contact angle α_A for three values of the friction coefficient which are possible in the technological problems considered above. The dimensionless radius of the plastic area is determined by the contact angle $r_A/R = \sin\alpha_A$.

Calculations show that the mean pressures on the punch in the case of Coulomb contact friction when $f = 0.05$ and Prandtl contact friction when $\mu = 0.1$ are close to one another for equal radii of the plastic area, but the sizes of the

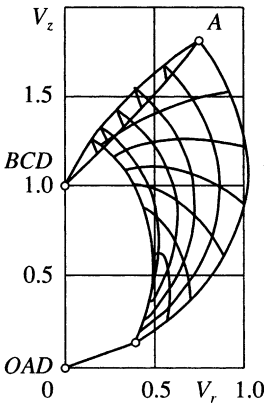

Fig. 5.

Table 1

α_A	q_M	q_B	$h/R\cdot10^4$	$-(z_E/R\cdot10^4)$	$r_G/R\cdot10^4$	q_M	q_B	$h/R\cdot10^4$	$-(z_E/R\cdot10^4)$	$r_G/R\cdot10^4$
$\mu=0.1$						$\mu=0.2$				
0.1	2.86	2.85	33	54	62	2.93	2.92	34	193	254
0.2	2.78	2.71	131	73	79	2.87	2.84	134	279	361
0.3	2.70	2.64	291	89	106	2.80	2.74	298	328	424
0.4	2.62	2.51	510	99	113	2.73	2.62	521	349	444
0.5	2.54	2.38	782	111	125	2.63	2.50	798	370	468
$f=0.05$										
0.1	2.88	2.88	34	134	168					
0.2	2.80	2.78	133	198	247					
0.3	2.72	2.66	295	242	300					
0.4	2.64	2.53	514	275	341					
0.5	2.55	2.40	793	280	333					

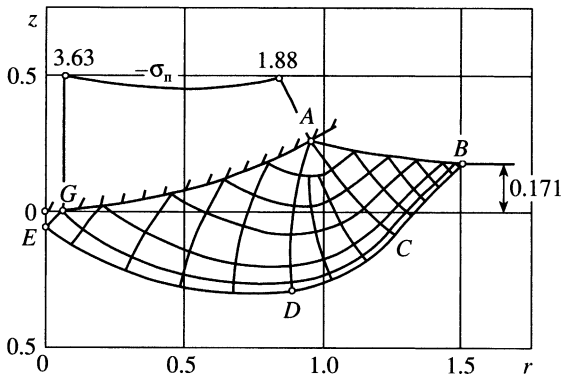

Fig. 6.

central rigid zone under the punch are much higher in the case of Coulomb contact friction than in the case of Prandtl contact friction.

The slip lines in the $\{r, z\}$ plane and their mapping onto the displacement velocity hodograph V_r and V_z in the case of the indentation of a spherical punch up to a contact angle $\alpha_A = 0.5$ with a Coulomb friction coefficient $f = 0.05$ are shown in Figs. 6 and 7. The slip line fields and the displacement velocity hodographs in the case of Coulomb contact friction and Prandtl contact friction when $\mu = 0.1$ hardly differ. However, the dependence of the contact shear stress

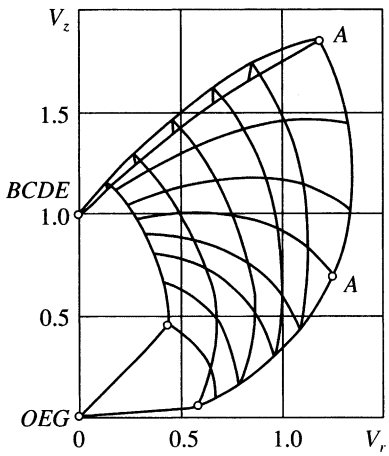

Fig. 7.

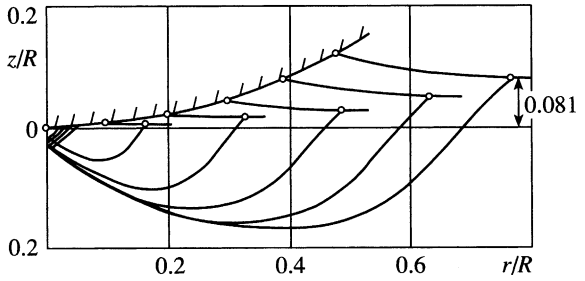

Fig. 8.

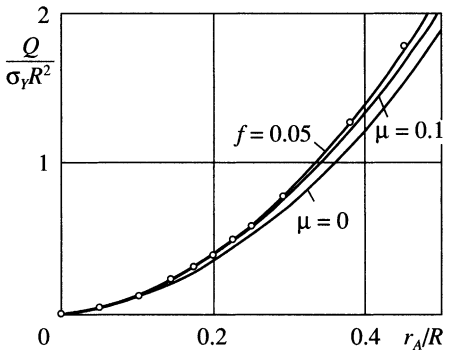

Fig. 9.

on the pressure in the case of Coulomb friction leads to a reduction in the angle of inclination of the slip lines η to the punch boundary and the formation of a central rigid zone with larger dimensions. The condition that the dissipative function must be non-negative is also satisfied in the example considered. The distribution of the contact pressure σ_n in the slip boundary AG is shown in the upper part of Fig. 6. This pressure increases from 1.876 at point A to 3.632 at point G. At the same time, the shear contact friction stress also increases from 0.0936 at point A to 0.1816 at point G.

The change in the boundaries of the plastic region and the central rigid zone when the punch is indented up to a contact angle $\alpha_A = 0.5$ in the case of a Prandtl friction coefficient $\mu = 0.2$ is shown in Fig. 8. At the beginning of the indentation of the punch at small contact angles, the free boundary AB only deviates slightly from a horizontal line. The slip line field in this region, including a flat punch when $\alpha_A = 0$, and the contact stress distribution are identical within the limits of the error of the numerical calculations with the solutions of the problem of the initial flow of a half-space with a horizontal boundary.[1–4]

A comparison of the calculated dependences of the dimensionless indentation force $Q/(\sigma_Y R^2)$ on the radius of the plastic area in the case of a smooth punch when $\mu = 0$ and punches with a Prandtl friction coefficient $\mu = 0.1$ and a Coulomb friction coefficient $f = 0.05$ (the solid lines) with experimental data on the indentation of a polished tungsten carbide ball into prehardened copper[6] (the open circles) is shown in Fig. 9. The yield stress σ_Y was found using the experimental relation[6] $\sigma_Y(\varepsilon_p)$ with the average values of the accumulated plastic deformation ε_p presented earlier in Ref. 5. When $r_A/R < 0.3$, the calculations using the present model were practically identical to the experimental data and to calculations of the indentation of a smooth punch into a half-space with a linear boundary.[1,3,4] As the radius of plastic area increases, the experimental data are in good agreement with the calculated values obtained taking account of contact friction when $\mu = 0.1$ and $f = 0.05$. The relation obtained earlier[1,3,4] is practically identical to the relation for $\mu = 0.1$ and astonishingly close to the experimental data. The horizontal boundary of the half-space assumed in Refs. 1,3,4, as well as contact friction, leads to an increase in the pressure on the punch compared with the calculations for a smooth punch.

References

1. Ishlinskii AYu. An axisymmetric problem in the theory of plasticity and the Brinell test. *Prikl Mat Mekh* 1944;**8**(3):201–24.
2. Ishlinskii AYu. *Applied Problems in Mechanics*, Vol. 1. Moscow: Nauka; 1986.
3. Ishlinskii AYu, Ivlev DD. *The Mathematical Theory of Plasticity*. Moscow: Fizmatlit; 2001.

4. Ivlev DD, Nepershin RI. The indentation of a smooth spherical punch into a rigid-plastic half-space. *Izv Akad Nauk SSSR MTT* 1973;**4**:159–66.
5. Nepershin RI. The indentation of a smooth spherical punch into an ideally plastic half-space. *Dokl Ross Akad Nauk* 2003;**389**(5):616–20.
6. Richmond O, Morrison HL, Devenpeck ML. Sphere indentation with application to the Brinell hardness test. *Intern J Mech Sci* 1974;**16**(1):75–82.
7. Shield RT. On the plastic flow of metals under condition of axial symmetry. *Proc Roy Soc London* 1955;**A 233**(1193):267–87.
8. Druyanov BA, Nepershin RI. *Theory of Technological Plasticity*. Moscow: Mashinostroyeniye; 1990.
9. Druyanov BA, Nepershin RI. *Problems of Technological Plasticity*. Amsterdam: Elsevier; 1994. p. 426.
10. Tomlenov AD. *Theory of the Plastic Deformation of Metals*. Moscow: Metallurgiya; 1972.
11. Sokolovskii VV. *The Theory of Plasticity*. Moscow: Vysshaya Shkola; 1969.
12. Dennis JE, Shnabel RB. *Numerical Methods for Unconstrained Optimization and Nonlinear Equations*. Englewood Cliffs, NJ: Prentice-Hall; 1983. p. 378.
13. Eason G, Shield RT. The plastic indentation of a semi-infinite solid by perfectly rough circular punch. *ZAMP* 1960;**T 11**(1):33–43.

Translated by E.L.S.